Two-Step Photon Absorption Driving the Chemical Reaction in the Model Ruthenium Nitrosyl System $[Ru(py)_4Cl(NO)](PF_6)_2.1/2\ H_2O$.

Liya Khadeeva #, Wawrzyniec Kaszub #†, Maciej Lorenc #, Isabelle Malfant §*, and Marylise Buron-Le Cointe #*.

Institut de Physique de Rennes, UMR UR1-CNRS 6251, Université Rennes 1, avenue du général Leclerc, 35042 Rennes, Cedex, FRANCE.

§ Laboratoire de Chimie de Coordination, CNRS UPR 8241, 205 route de Narbonne, 31077 Toulouse Cedex, FRANCE.

Supporting Information:

Contents:

Figure S5. Evolution of the OD during the light irradiation of the $[Ru(py)_4Cl(NO)](PF_6)_2.1/2H_2O$ single crystal at 100 K with 1064 nm, 600 $mW.cm^{-2}$ up to $MSII^{IR}$ (black thick line) and then (a) with 473 nm, around 1100 $mW.cm^{-2}$, (b) with 532 nm, around 1500 $mW.cm^{-2}$. $MSII^{IR}$ indicates the highest population of MSII species reached during the experiment.

Figure S6. Agreement between the experimental data (points) and the three state (GS, MSI and MSII) kinetic model for reproducing the experimental intermediate OD spectra during the GS to MSI photo-transformation. View in 3D.

Scheme S1. Relative positions of the MSI and MSII states of $[Ru(py)_4Cl(NO)]^{2+}$ complex, their excited states and excited level of the GS state. (From Ref [19]). Arrows represent green, 532 nm, irradiation. The red numbers stand for the calculated values, while the black ones for the measured values.

Experimental section:

Visible absorption spectroscopy. Absorption spectra of single crystals were collected by home-made spectrograph able to cover visible range with accuracy down to $d\lambda$ = 5nm. Dedicated wavelength was choosen by monochromator (Digikröm CM110) equipped with the slit 0,6 mm, seeded by the halogen lamp (Spectral Products, model: ASBN-W150). Higher orders of the diffraction grating are rejected. Probe light was mechanically chopped down to 500 Hz and focused on the sample by home-made objective with spot size of the image of the halogen lamp filament around 150 × 300 μm^2, while the typical size of the investigated crystal was 450 × 500 μm^2 for a thickness of about 100 µm. Spectral changes of transmitted light were detected by photodiode (Thorlabs DET10, DET36) and correlated with the reference signal recorded by second photodiode (reference, Thorlabs DET10, DET36) measuring copied by the beam splitter signal before sample. Signals from photodiodes were transferred to computer via two Lock-In Amplifiers synchronized with the chopper (Thorlabs). Single measurement was controlled by LabView software correlating signals from detection system with monochromator setup and recording one spectrum in one file. The measurements were done at room temperature and at low temperatures, 100 K, 140 K, 180 K, where crystals were cooled down by CryoJet system from Oxford Crogenics (CryoJet 700). To study the photo-induced phenomena the crystals were irradiated with diode lasers (473 nm, 532 nm, 782 nm, and 1064 nm). Precise determination of the laser powers was done using a combination of laser beam profiler (Spiricon SP620U) and pyroelectric measurements (Melles Griot Broadband power meter 13PEM001). The FWHM width of the gaussian laser profile was measured and the power delivered per cm^2 was deduced after taking into account the 0.76 factor between the power delivered within this FWHM width and the total power considering the whole gaussian beam.

X-Ray diffraction. Structural investigations under continuous light irradiation were performed by X-ray diffraction on single crystals (473 nm, 280 $mW.cm^{-2}$; 1064 nm, 130 $mW.cm^{-2}$). Data were collected on a four-circle Oxford Diffraction Xcalibur 3 diffractometer (MoK_α radiation) with a 2D Sapphire 3 CCD detector, on samples with typical sizes around 300 × 200 × 100 μm^3. The single crystals were mounted in an Oxford Cryosystems nitrogen-flow cryostat allowing a precise control of temperature at 100 and 140 K. The unit cell parameters and the data reduction were obtained with CrysAlis software from Oxford Diffraction[i]. All unit-cell parameter values are collected under light irradiation and each point corresponds to a time-average value of ten minutes. The structures were solved with SIR-97[ii] and refined with SHELXL[iii]. Structure refinement of the GS state and MSI one (or mixed GS-MSI) gives a final R1 factor equal to 0.0387 and 0.0384 respectively [iv].

Polarization effect. The study of the light polarization effect was carried out in ruthenium nitrosyl complex to see if there is a strong influence on the MSI population as in prototype SNP compound.

The visible absorption spectroscopy was performed with the use of the Berek Polarization Compensator on (ab) platelets. It was found that the polarization of the laser light, either parallel to **a** or parallel to **b** crystallographic axis does not play any significant role in the Ru-NO to Ru-ON photoswitching of the ruthenium nitrosyl system (identical final OD spectra in both cases).
For the X-Ray studies polarization of the laser beam is not important as the crystal is rotated along different axes during the data collection. Evolution of unit-cell parameters are collected with light on.

Kinetic model: For Ru-NO to Ru-ON photoswitching process, the following kinetic model with one intermediate state and exponential growth and decay was probed:

$A \overset{k_1}{\rightarrow} B \overset{k_2}{\rightarrow} C$, with the rate equations $\frac{dA}{dt} = -k_1 A$, $\frac{dB}{dt} = k_1 A - k_2 B$, $\frac{dC}{dt} = k_2 B$.

The model takes into account the two-step process with the following kinetic constants: $k_1 = K_{GS \rightarrow MSII}$, $k_2 = K_{MSII \rightarrow MSI}$. The kinetic constants are free parameters which are found in the data fitting.

For the analysis we consider that the experimental data can be presented as follows:

$$D(\lambda, \tau) = P(\tau) \cdot B(\lambda),$$

where $D(\lambda, \tau)$ is a matrix of spectral data points at a certain wavelength λ and time τ, $B(\lambda)$ is a matrix containing the basic spectra and $P(\tau)$ shows the populations in each basic spectra. The basic spectra consist of three components: two known spectra of GS and MSI taken from the measurements, and the spectrum of MSII state deduced from the OD evolution. Following the assumption above we can present the basis and the expected data as below:

$$B = (P_M^T \cdot P_M)^{-1} \cdot P_M^T \cdot D$$
$$D_M = P_M \cdot B$$

where subscript M stands for the model used. During the fitting procedure we verify the goodness of fit of the experimental data to the expected one by chi-squared tests, $\chi^2 = \sum_{\lambda,\tau} \left(\frac{D - D_M}{\sigma}\right)^2$.

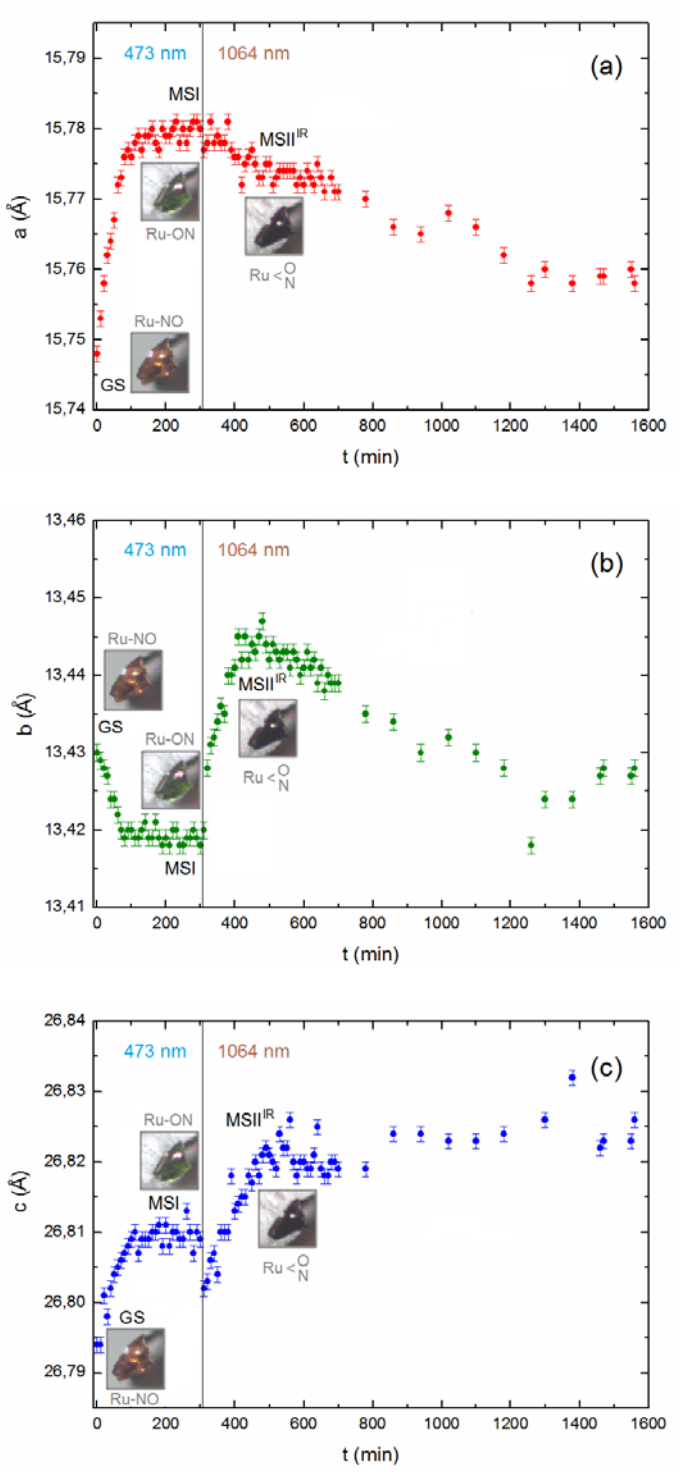

Figure S1. Evolution of the lattice parameters a, b and c during the light irradiation of the $[Ru(py)_4Cl(NO)](PF_6)_2.1/2H_2O$ single crystal at 100 K with 473 nm, around 280 $mW.cm^{-2}$ and then 1064 nm, around 130 $mW.cm^{-2}$.

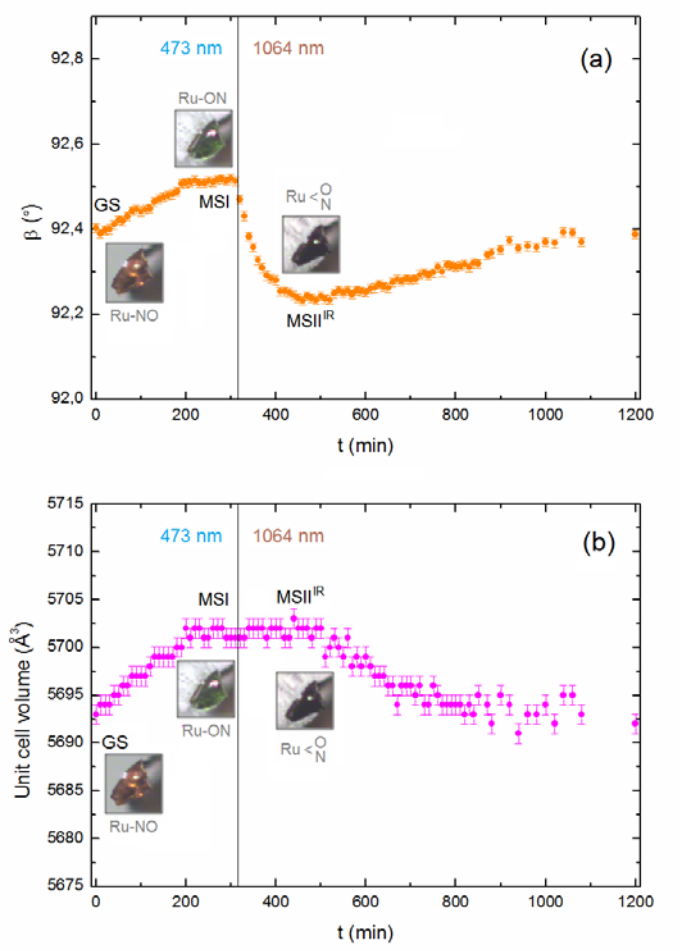

Figure S2. Time evolution of (a) the β angle (degree) and (b) unit cell volume when first using 473 nm, (280 mW.cm^{-2}) (Ru-NO to Ru-ON photo-switching) and second using 1064 nm, 130 mW.cm^{-2} (Ru-ON to Ru-NO photoswitching through MSII state) at 140 K.

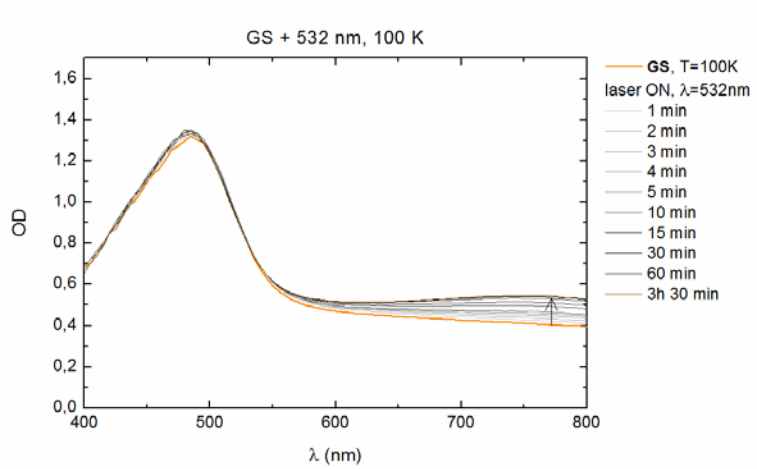

Figure S3. Evolution of the OD during the light irradiation of the $[Ru(py)_4Cl(NO)](PF_6)_2.1/2H_2O$ single crystal at 100 K with 532 nm, around 1500 $mW.cm^{-2}$.

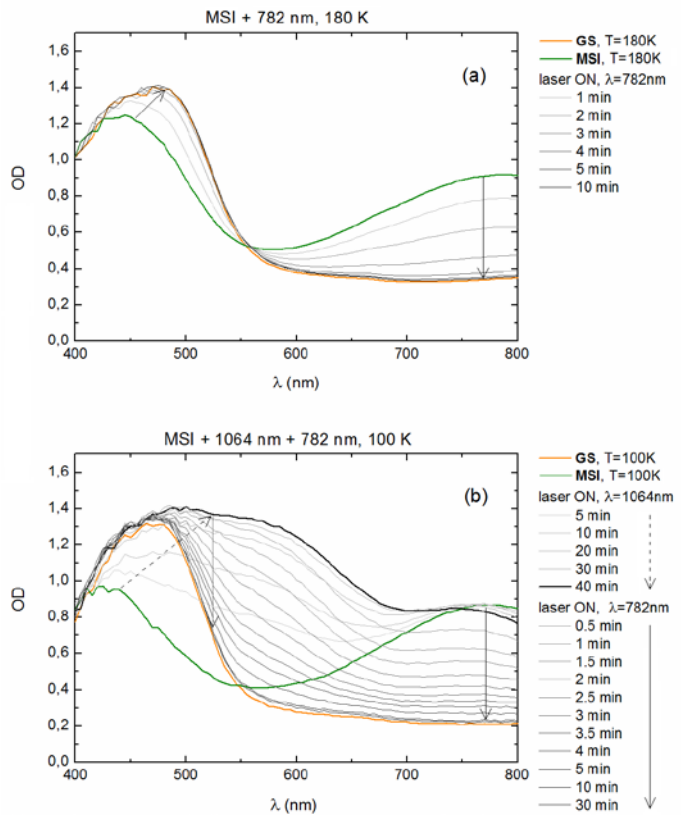

Figure S4. (a) Evolution of the OD during the light irradiation of the $[Ru(py)_4Cl(NO)](PF_6)_2.1/2H_2O$ single crystal with 782 nm, 180 $mW.cm^{-2}$ at 180 K. (b) Evolution of the OD during the light irradiation of the $[Ru(py)_4Cl(NO)](PF_6)_2.1/2H_2O$ single crystal with 1064 nm, 600 $mW.cm^{-2}$ up to $MSII^{IR}$ (black thick line) and then with 782 nm, 180 $mW.cm^{-2}$ at 100 K. $MSII^{IR}$ indicates the highest population of MSII species reached during the experiment.

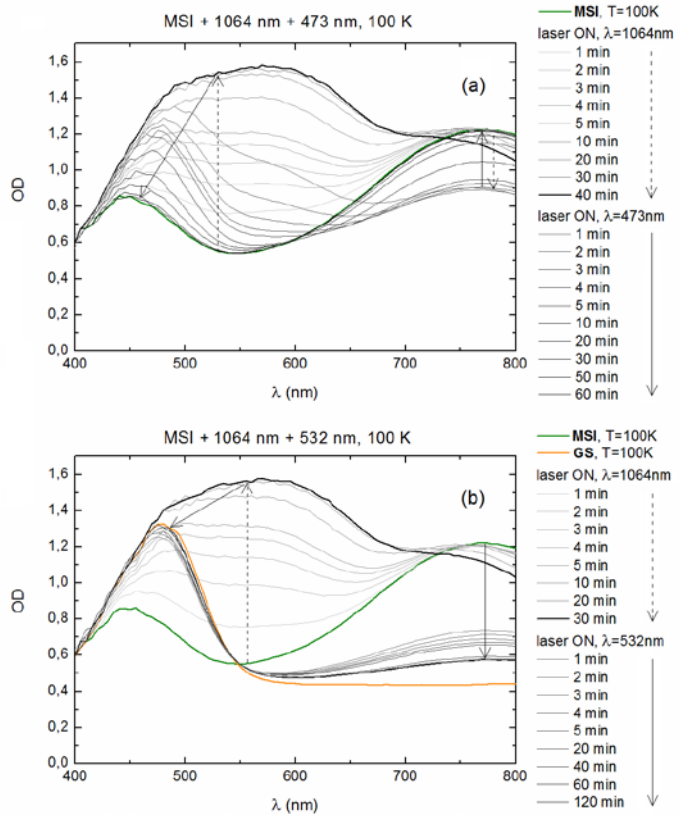

Figure S5. Evolution of the OD during the light irradiation of the $[Ru(py)_4Cl(NO)](PF_6)_2.1/2H_2O$ single crystal at 100 K with 1064 nm, 600 mW.cm^{-2} up to MSII^{IR} (black thick line) and then (a) with 473 nm, around 1100 mW.cm^{-2}, (b) with 532 nm, around 1500 mW.cm^{-2}. MSII^{IR} indicates the highest population of MSII species reached during the experiment.

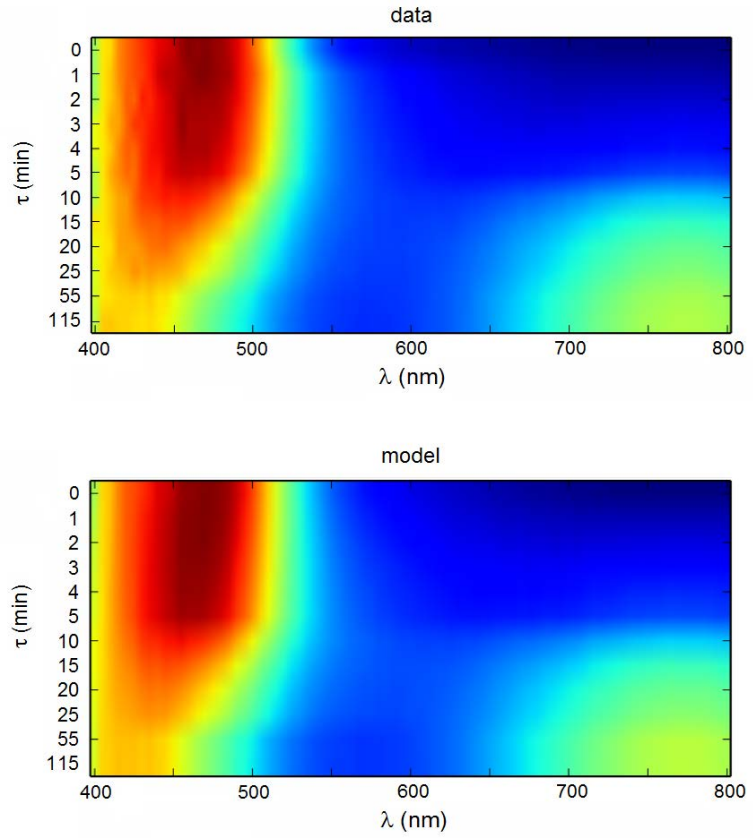

Figure S6. Agreement between the experimental data (points) and the three state (GS, MSI and MSII) kinetic model for reproducing the experimental intermediate OD spectra during the GS to MSI photo-transformation. View in 3D.

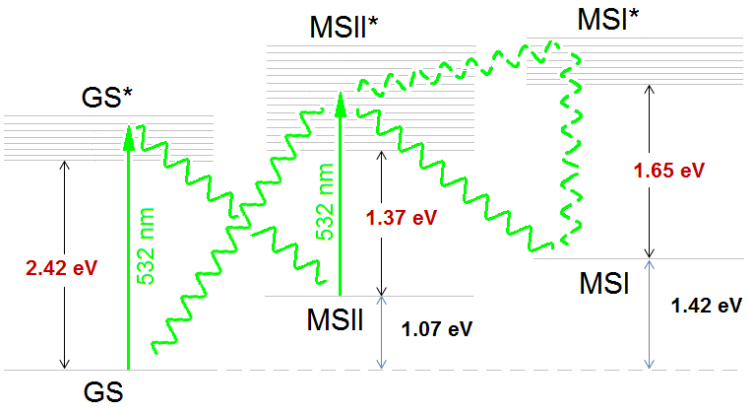

Scheme S1. Relative positions of the MSI and MSII states of $[Ru(py)_4Cl(NO)]^{2+}$ complex, their excited states and excited level of the GS state. (From Ref [19]). Arrows represent green, 532 nm, irradiation. The red numbers stand for the calculated values, while the black ones stand for the measured values.

---

[i] CrysAlis RED, Oxford Diffraction Ltd, Version 1.171.32.5 (2007).

[ii] A. Altomare, M.C. Burla, M. Camalli, G. Cascareno, C. Giacovazzo, A. Guagliardi, A. G. G. Moliterni, G. Polidori, and R. Spagna J. Appl. Cryst. **32**, 115 (1999).

[iii] G. M. Sheldrick, Acta Cryst. A64, 112 (2008).

[iv] CCDC-1040140 (GS), CCDC-1040141 (mixed GS-MSI) and CCDC-1040190 (MSI) contain the supplementary crystallographic data for this paper. These data can be obtained free of charge via www.ccdc.cam.ac.uk/conts/retrieving.html (or from the Cambridge Crystallographic Data Centre, 12 Union Road, Cambridge CB21EZ, UK; fax: (+44) 1223-336033; or deposit@ccdc.cam.uk).